

Silver nanoparticles: cytotoxic, apoptotic, and necrotic effects on MCF-7 cells

Hakan ÇİFTÇİ¹, Mustafa TÜRK^{2,3,*}, Uğur TAMER⁴, Siyami KARAHAN^{3,5}, Yusuf MENEMEN⁶

¹Department of Chemistry and Chemical Processing Technologies, Kırıkkale Vocational High School, Kırıkkale University, Yahşihan, Kırıkkale, Turkey

²Department of Bioengineering, Faculty of Engineering, Kırıkkale University, Yahşihan, Kırıkkale, Turkey

³Kırıkkale University Scientific and Research Laboratories, Yahşihan, Kırıkkale, Turkey

⁴Department of Analytical Chemistry, Faculty of Pharmacy, Gazi University, Ankara, Turkey

⁵Department of Histology and Embryology, Faculty of Veterinary Medicine, Kırıkkale University, Yahşihan, Kırıkkale, Turkey

⁶Department of Biology, Faculty of Sciences and Arts, Kırıkkale University, Yahşihan, Kırıkkale, Turkey

Received: 06.02.2013 • Accepted: 05.04.2013 • Published Online: 06.09.2013 • Printed: 04.10.2013

Abstract: The present study was conducted to examine cytotoxic, apoptotic, and necrotic effects of silver nanoparticles (AgNPs) on MCF-7 cells. Colloidal AgNPs were fabricated in an alkaline pH environment via reduction of silver nitrate with hydroxylamine hydrochloride. The size of AgNPs was measured by atomic force microscopy (AFM), transmission electron microscopy (TEM), and dynamic light scattering. Zeta potential of AgNPs was determined by laser Doppler microelectrophoresis. After exposing MCF-7 cells to AgNPs for 24 h, cytotoxicity was measured by WST-1 assay. Apoptosis and necrosis in MCF-7 cells were detected by Annexin-V-FLUOS immunostaining and double staining of Hoechst dye with propidium iodide. In AFM and TEM analyses, the sizes of AgNPs varied from 16 nm to 20 nm. AgNPs were 80 nm in hydrodynamic diameter with a zeta potential of -38.2 mV. The WST-1 assay resulted in an IC₅₀ value of 40 μ g/mL. AgNPs caused apoptotic and necrotic effects in a dose-dependent manner. The apoptotic effect of AgNPs was marked up to a concentration of 80 μ g/mL AgNPs. At higher concentrations, the apoptotic effect decreased while the necrotic effect became prominent. The results indicate that AgNPs with a zeta potential of -38.2 mV and hydrodynamic diameter of 80 nm can be used in vitro at concentrations of up to 40 μ g/mL.

Key words: Silver, nanoparticle, MCF-7, cancer, apoptosis, necrosis, cytotoxicity

1. Introduction

Nanoparticles (NPs) of different size and physicochemical properties have been introduced to many fields of life and biomedical sciences over the last decade (Oberdörster et al., 2005). In this respect, NPs opened a new era in biomedical sciences and have been used specifically as gene or agent carriers, and in drug design, modification of therapeutics, labeling of fluorescents, and tissue engineering (Tan et al., 2007; Yoon et al., 2007; Kreuter and Gelperina, 2008; Su et al., 2008; Hackenberg et al., 2010).

Among the NPs, silver nanoparticles (AgNPs) have received attention for their antimicrobial activities (Cho et al., 2005; Kim et al., 2006) and have been used for different purposes including the manufacture of disinfectants, shampoos, deodorants, humidifiers, wound dressings, and various textile products (Ahmed et al., 2008; Johnston et al., 2010; Zanette et al., 2011); they have also been used as a coating for various implantable devices such as catheters, heart valves, and implants (Chen and Schluesener, 2008;

Chaloupka et al., 2010). Despite their benefits, there has been serious concern about the possible side effects of AgNPs. Previous studies reported that AgNPs induced genotoxicity and cytotoxicity in both cancer and normal cell lines (Yoon et al., 2007), altered cell morphology, reduced cell viability, and caused oxidative stress in lung fibroblast and glioblastoma cells (Asharani et al., 2009), human and rat liver cells (Hussain et al., 2005; Kim et al., 2010), HeLa cells (Sonoda et al., 1998), and THP-1 monocytes (Foldbjerg et al., 2009). AgNP-induced cytotoxicity reduces cell viability in various cell lines by causing apoptosis through the mitochondrial pathway (Hsin et al., 2008) and generates oxidant species (Hess et al., 2008), which are well known for causing lipid peroxidation of biological membranes and damage to structural proteins and DNA (Li and Osborne, 2008). Liu et al. (2010) reported that the cytotoxicity exerted by AgNPs is size-dependent, as smaller particles can enter cells easily. They found that AgNPs of ~ 5 nm in size

* Correspondence: mtrk.35@gmail.com

caused higher toxicity than those of ~20 nm and ~50 nm in size. The surface properties also affect entrance of AgNP into cells. Sur et al. (2012) modified AgNPs and citrate-reduced AgNPs with either lactose or a 12-base-long oligonucleotide. They determined that lactose-modified AgNPs caused more DNA damage in A549 cells compared to oligonucleotide-modified AgNPs. Furthermore, modification of citrate-reduced AgNPs increased their cytotoxicity. In another study, Sur et al. (2010) found that lactose-modified AgNPs enter the L929 cells at a higher rate, and differential uptake of AgNPs by cells was influenced by modification of AgNPs with oligonucleotide binding, along with carbohydrates. The biosafety- and cell toxicity-related issues of AgNPs are of scientific interest for the reasons mentioned above. In addition, determination of a tolerable AgNP concentration for in vitro use is important for various applications, including plasmonic photothermal therapy (PPTT) studies in cancer cells, for which AgNPs seem to be useful due to their smaller sizes but relatively larger surface areas (Oberley et al., 2006). Thus, the aim of the present study was to examine the cytotoxic, necrotic, and apoptotic effects of AgNPs on the human breast adenocarcinoma cell line (MCF-7), which is a well-established cell line and has been used in many studies, including drug resistance in cancers. A study by Liu et al. (2010) claimed that cytotoxicity on cell lines such as MCF-7 is influenced by size and surface area of AgNPs. However, the mechanisms of cytotoxicity on different cell lines, including their apoptotic, necrotic, and antiproliferative effects, remain to be investigated. The data generated in this study would serve as a basis for future studies.

2. Materials and methods

2.1. Materials

Silver nitrate (AgNO_3), hydroxylamine hydrochloride ($\text{NH}_2\text{OH}\cdot\text{HCl}$), and sodium hydroxide (NaOH) were commercially purchased from Merck (Darmstadt, Germany). All solutions were prepared in deionized water (Millipore, USA), which was $18.2 \text{ M}\Omega \text{ cm}$ free from organic matter.

MCF-7 cancer cells were obtained from the Division of Bioengineering of Istanbul University, Turkey. Cell culture flasks and other plastic materials were purchased from Corning (USA). Dulbecco Modified Eagle's Medium (DMEM) with L-glutamine, fetal calf serum (FCS), trypsin-EDTA, Hoechst 33342, and propidium iodide (PI) were purchased from Serva (Israel). Annexin-V-FLUOS was purchased from Roche (Germany).

2.2. Fabrication of silver nanoparticles

The colloidal AgNPs were fabricated through reduction of silver nitrate by hydroxylamine hydrochloride in an

alkaline pH environment at room temperature, according to a procedure previously published (Leopold and Lendl, 2003). Briefly, 10 mL of AgNO_3 suspension (10^{-2} M) was rapidly added to 90 mL of freshly prepared $\text{NH}_2\text{OH}\cdot\text{HCl}$ solution ($1.67 \times 10^{-3} \text{ M}$) containing $3.33 \times 10^{-3} \text{ M}$ NaOH (10^{-1} M solution) while stirring. The fabricated colloidal AgNPs (10^{-3} M) were kept for 3 weeks at room temperature in a dark place. The fabricated AgNPs, in physiologic saline, were centrifuged at 13,000 rpm 3 times. Fresh physiologic saline was used each time.

2.3. Nanoparticle characterization

Optical absorption spectra of AgNPs were collected within a range of 300–800 nm using optical absorption spectroscopy (Thermo Spectronics Genesys, USA). This model is a single-beam spectrophotometer using 1-cm path length quartz cuvettes. The size and size distribution analyses were conducted using an atomic force microscope (AFM) (Scanning Probe Microscope, Park Scientific Instruments, Korea). Transmission electron microscopy (TEM) analyses were performed on a JEOL 2100 HRTEM instrument (JEOL Ltd., Japan) to determine particle diameter using a Zeta Sizer-Nano ZS (Malvern Instruments, UK). The hydrodynamic diameter of AgNPs was measured by dynamic light-scattering, and zeta potential was determined by laser Doppler microelectrophoresis.

2.4. Cell culture for MCF-7 cells

MCF-7 cells were placed in flasks containing DMEM with L-glutamine, 10% FCS, and 1% antibiotic and were kept in a CO_2 incubator conditioned with 5% CO_2 at 37°C for 48 h. For harvesting cells, the cell culture medium was discharged, and the cells were treated with trypsin-EDTA (0.5 mL per flask). Cells were then transferred into 15-mL Eppendorf tubes and centrifuged at 1000 rpm for 3 min. The supernatant was discharged and the cells were used in the prospective studies.

2.5. WST assay for cytotoxicity

MCF-7 cells (5×10^3 cells per well) were placed in 96-well plates containing DMEM with L-glutamine, 10% FCS, and 1% antibiotic. The plates were then kept in a CO_2 incubator (37°C in 5% CO_2) for 24 h, after which time, when the cells attached to the bottom of the plate, the cell culture medium was replaced with fresh medium and different concentrations (10–120 $\mu\text{g}/\text{mL}$ in aqueous suspensions) of AgNPs were placed into the wells. Following incubation under the same conditions for an additional 72 h, WST-1 (a water-soluble tetrazolium salt) reagent (15 μL) was added into each well. Upon incubation for an additional 4 h, the plates were immediately read in an Elisa Microplate Reader (BioTek, USA) at 440-nm and 630-nm reference wavelengths.

2.6. Cell proliferation assay

Cell proliferation was determined using a Real-Time Analyzer (RTCA) SP Instrument (Roche, Germany) to monitor cell proliferation after treatment with AgNPs *in vitro*. MCF-7 cells (10×10^3 cells per well) were cultivated in DMEM-F12 without L-glutamine, using E-Plate 96 (Roche) for cell-growth monitoring. The plates were kept in a CO₂ incubator (37 °C in 5% CO₂) during the experiment. At hour 21 of incubation, different concentrations of AgNPs (10, 20, 40, 80, and 120 µg/mL in medium) were added to the wells containing MCF-7 cells and cultivated under the same conditions mentioned above. For control groups, cell culture medium was added instead of AgNPs. The attachment and logarithmic growth of the cells was measured every 10 min over 42 h.

2.7. Analysis of apoptotic and necrotic cells

Double staining of Hoechst dye with PI was performed to quantify the number of apoptotic and necrotic cells in culture on the basis of scoring cell nuclei. MCF-7 cells (10×10^3 cells per well) were grown in DMEM-F12 with L-glutamine supplemented with 10% fetal calf serum and 1% penicillin-streptomycin at 37 °C in a 5% CO₂ humidified atmosphere in 48-well plates. MCF-7 cells were treated with different concentrations of AgNPs (10–200 µg/mL) for 24 h. The control group consisted of MCF-7 cells treated with cell medium only. Both attached and detached cells were collected, then washed with phosphate-buffered saline (PBS) and stained with Hoechst dye 33342 (2 mg/mL), PI (2 µg/mL), and DNase free-RNase (100 µg/mL) for 15 min at room temperature. Next, 10–50 µL of cell suspension was smeared onto a glass slide for examination by fluorescence microscope (Leica, Germany). With the Hoechst dye, the nuclei of normal cells were stained with blue fluorescence of low intensity, but apoptotic cells were stained a stronger blue fluorescence. The apoptotic cells were also identified by morphological changes in the nucleus including nuclear fragmentation and chromatin condensation (van Engeland et al., 1998; Türk et al., 2010). Nuclei of necrotic cells were stained red by PI, as PI dye can cross the cell membrane of necrotic cells, which lack plasma membrane integrity. The PI dye cannot cross the nonnecrotic cell membrane (Kamphaus et al., 2000; Tice et al., 2000). The numbers of apoptotic and necrotic cells were counted at 10 randomly chosen microscopic fields using the 40× microscope objective. The number of apoptotic and necrotic cells were determined using a DMI600 Fluorescence Inverted Microscope (Leica, Germany) with DAPI and FITC filters, respectively. Data were expressed as a ratio of apoptotic or necrotic cells to normal cells.

Annexin-V-FLUOS, a calcium-dependent phospholipid-binding protein with a high affinity for phosphatidylserine (PS), was used to detect apoptosis. The Annexin-V-FLUOS assay takes advantage of the fact that

PS translocates from the inner (cytoplasmic) leaflet of the plasma membrane to the outer (cell surface) leaflet soon after the induction of apoptosis, and that the Annexin V protein has a strong, specific affinity for PS (Tan et al., 2007; Yoon et al., 2007; Su et al., 2008). The PS on the outer leaflet is available to bind labeled Annexin V, providing the basis for a simple staining assay (van Engeland et al., 2008). Briefly, MCF-7 cells (10×10^3 /well) were seeded into a 48-well plate with DMEM including 10% FCS. The next day, the medium was discharged and replaced with fresh medium containing 10% FCS and AgNPs ranging from 10 µg/mL to 120 µg/mL. In the control group, MCF-7 cells were treated with cell culture medium only. After 24 h of treatment, cell culture medium containing floating cells was collected and centrifuged at 3000 rpm. Adherent cells were stained in the well. The cells were then washed in PBS and resuspended in binding buffer (10 mM HEPES/NaOH, pH 7.4, 140 mM NaCl, 2.5 mM CaCl₂). Annexin-V-FLUOS (Roche) and PI were added to final concentrations of 10 µg/mL and 1 µg/mL, respectively, and the cells were incubated in the dark for 10 min. The cells were washed again in PBS and resuspended in binding buffer. The numbers of Annexin-V-FLUOS-labeled cells were counted using the 40× objective of an inverted fluorescence microscope (Leica DMI6000, Germany). For each image, 3 randomly selected microscopic fields were evaluated.

3. Results

3.1. Characterization of silver nanoparticles

Optical properties of AgNPs were determined by the excitation of plasmon resonances. Figure 1A illustrates the typical UV-Vis spectrum of silver nanoparticles. The UV-Vis absorption spectrum shows an intense absorption peak around 420 nm, originating from the surface plasmons' absorption of nanosized AgNPs. Under the conditions used for fabrication, AgNPs had a relatively narrow size distribution around 20 nm and 80 nm (Figure 1B), formed stable dispersions, and were negatively charged. The zeta potential value was -38.2 mV, which is a characteristic property of stable colloids. In the zeta analysis, the suspension of nanoparticles consisted of particles with an average size of 80 nm in hydrodynamic diameter. Figure 1C illustrates an AFM image of AgNPs, performed on a scanning probe microscope in tapping mode under ambient conditions. The AgNPs were dropped onto freshly cleaved mica. Most of the nanoparticles ranged from 16 to 20 nm in size. The average size of the particles on the substrates was 18 nm with a standard deviation of 2 nm. AFM indicated that AgNPs were spherical and relatively uniform. Figure 1D displays TEM images of the spherical silver nanoparticles. The spherical AgNPs have uniform morphology, with an average diameter of 17 nm.

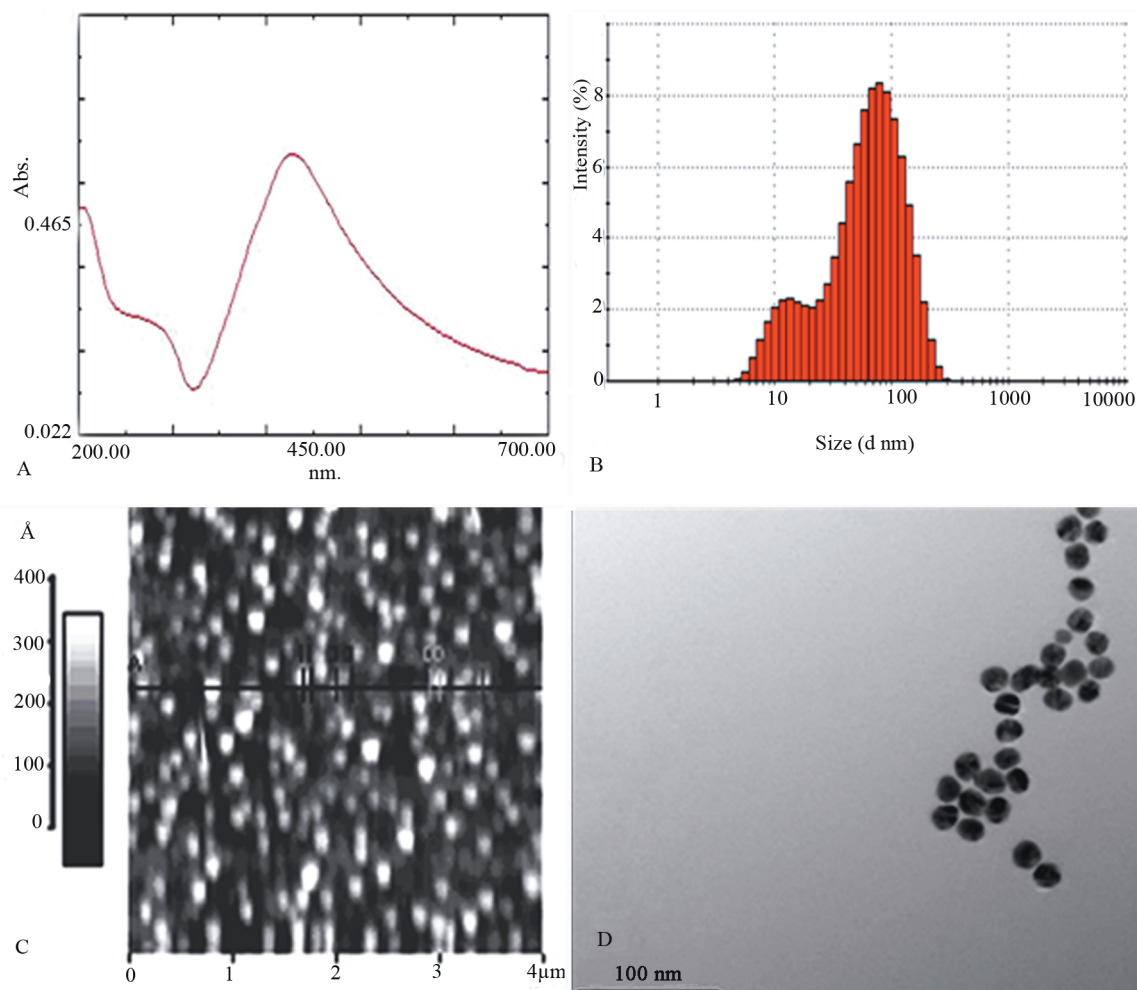


Figure 1. Characterization data of AgNPs: A) UV-Vis spectrum of silver nanoparticles; B) particle-size distribution histogram of silver nanoparticles; C) atomic force microscope image of silver nanoparticles; and D) transmission electron microscope images of spherical silver nanoparticles.

3.2. Cytotoxicity

MCF-7 cells exposed to AgNPs had alterations in cell shape and morphology, whereas control cells exhibited no change in morphology. According to WST assay results, nanoparticle concentrations significantly affected their impact on cell viability in a concentration-dependent manner (Table 1). The lowest mortality rate was obtained at a nanoparticle concentration of 10 $\mu\text{g}/\text{mL}$, whereas the highest mortality rate was obtained at 120 $\mu\text{g}/\text{mL}$, which was the highest concentration tested (Table 1). AgNPs were cytotoxic on MCF-7 cells with a half-maximal inhibiting concentration value (IC_{50}) of 40 $\mu\text{g}/\text{mL}$ (Table 1).

3.3. Cell proliferation effect of AgNPs

Antiproliferative effects of AgNPs were evaluated on MCF-7 cells line based on the RTCA system results. Figure 2 illustrates the cell index, indicating proliferation rate of MCF-7 cells. The antiproliferative effect was observed

Table 1. Cytotoxic effects of varying concentrations of silver nanoparticles (NPs) on the MCF-7 cell line revealed by WST assay. The cell viability (%) based on mean absorbance values at 440 nm is presented. Data are expressed as mean \pm standard error as calculated from 3 separate experiments.

Amount of NP in a well ($\mu\text{g}/\text{mL}$)	Cell viability (%)
0	98 \pm 0.12
10	75.56 \pm 4.75
20	57.29 \pm 2.12
40	48.7 \pm 3.73
80	31.45 \pm 3.19
120	15.63 \pm 4.58

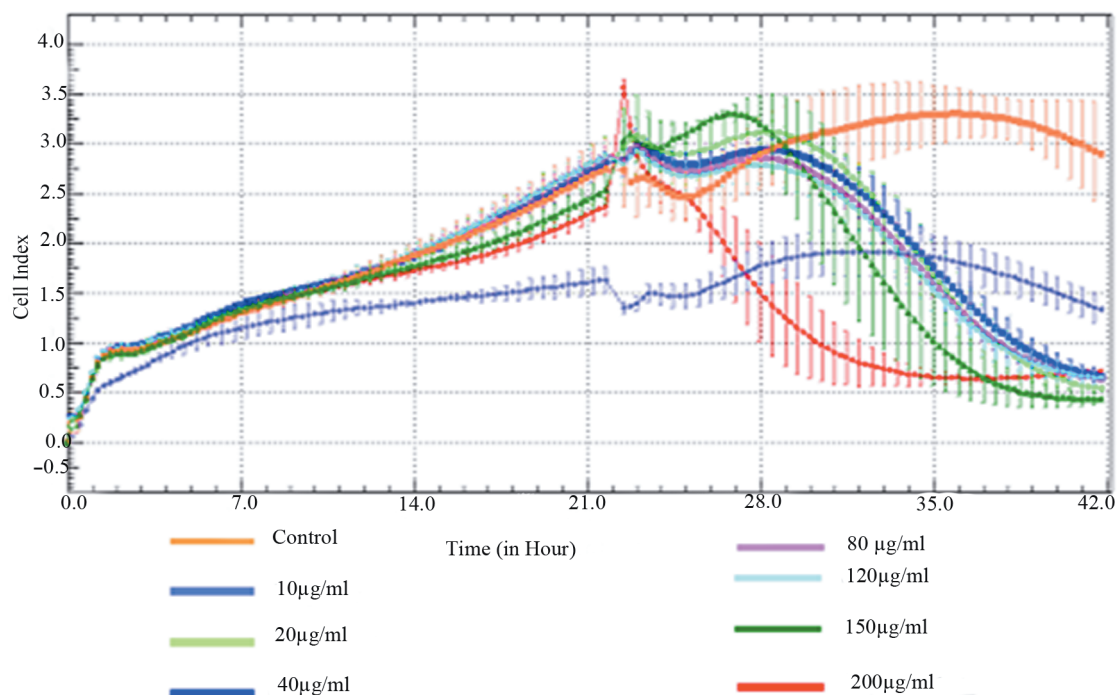


Figure 2. Dynamic monitoring of MCF-7 cells treated with AgNP using the Real-Time Analyzer (RTCA) SP. Cell index was monitored every 10 min for 42 h. At hour 21 of incubation, cells were exposed to AgNPs (10 to 120 µg/mL) in E-Plates 96. Controls include only medium.

2 h after inoculating AgNPs into wells. AgNPs inhibited MCF-7 cell proliferation in a concentration-dependent manner. However, cell proliferation in control groups kept increasing for another 22 h, at which time the test was stopped.

3.4. Analysis of apoptotic and necrotic cells

Table 2 illustrates the apoptotic index obtained from the double staining of Hoechst and PI as well as from Annexin-V-FLUOS staining. Figure 3 illustrates the normal, apoptotic, and necrotic cells under a fluorescent inverted microscope. In the control group, no morphological

changes were seen in the cell nuclei (Figure 3A). However, the apoptotic cell nuclei were stained with a stronger blue fluorescence compared to nonapoptotic cells (Figure 3B). The apoptotic effect in Annexin-V-FLUOS staining can be seen clearly, especially in wells containing 40 µg/mL of AgNPs (Figure 3C). Figure 3D represents the fluorescent-light micrograph without the fluorescent filter taken from the same area as Figure 3C to show cell morphology. The apoptotic indexes indicated that AgNPs exhibited an apoptotic effect in a concentration-dependent manner up to 40 µg/mL of concentration (Table 2). When the

Table 2. Apoptotic and necrotic indexes obtained from MCF-7 cell cultures following incubation with different concentrations of silver nanoparticles (NP). Data are expressed as mean ± standard error as calculated from 3 separate experiments.

Amount of NP in a well (µg/mL)	Apoptotic index (%)	Necrotic index (%)
0	2 ± 1	1 ± 1
10	12 ± 2	20 ± 4
20	18 ± 3	35 ± 3
40	28 ± 3	42 ± 4
80	24 ± 2	53 ± 3
120	20 ± 1	69 ± 2

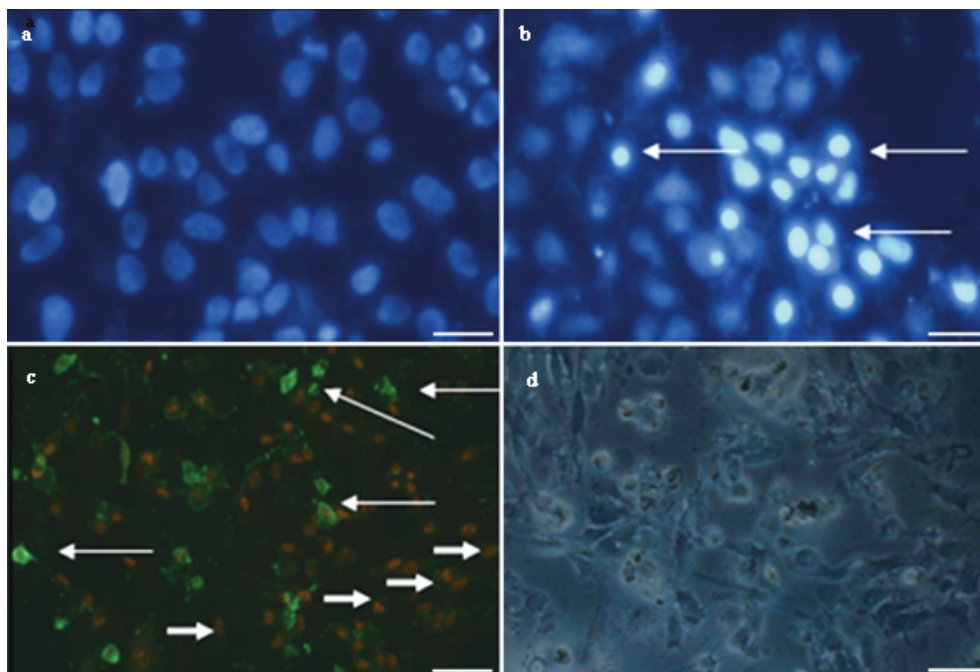


Figure 3. Apoptotic and necrotic cells in normal and silver nanoparticle-treated MCF-7 cell cultures, obtained from Annexin-V-FLUOS staining and double staining of Hoechst 33342 with propidium iodide. a) In the control group, MCF-7 cells did not express apoptotic and necrotic features, as the cell nuclei exhibited blue fluorescence of low intensity with Hoechst 33342 dye and cell borders were normal without decomposition of nuclear integrity. b) Apoptotic MCF-7 cells can be identified easily with their stronger blue fluorescence staining (arrows) obtained in wells exposed to AgNPs (40 $\mu\text{g}/\text{mL}$). c) In Annexin-V-FLUOS staining, apoptotic MCF-7 cells appeared green in color (long arrows) when exposed to AgNPs (40 $\mu\text{g}/\text{mL}$), while necrotic cells had red nuclear staining (short arrows). d) This micrograph was taken from the same area as in Figure 3C, without using the fluorescent filter. Microphotographs were taken with a Leica inverted fluorescent microscope DMI6000. All scale bars = 40 μm .

concentration of AgNPs was increased to 80 and 120 $\mu\text{g}/\text{mL}$, the apoptotic indexes gradually decreased, but the necrotic effect became more prominent. The necrotic effect induced by AgNPs on MCF-7 cancer cells is presented in Table 2. The necrotic effect was highly concentration-dependent. The necrotic cell percentages were $20 \pm 4\%$ and $69 \pm 2\%$ at 10 $\mu\text{g}/\text{mL}$ and 120 $\mu\text{g}/\text{mL}$ concentrations of AgNPs, respectively.

4. Discussion

Silver nanoparticles are metallic nanostructures with useful surface properties and have been used for various purposes, such as the production of wound dressings and cosmetics, and in the medical industry as device-coating agents (Tian et al., 2007; Wijnhoven et al., 2009). However, many studies showed that AgNPs may induce genotoxicity and cytotoxicity in cancer and normal cell lines (Yoon et al., 2007). In the present study, AgNPs were also determined to be cytotoxic to some degree on MCF-7 cancer cells with an IC_{50} value of 40 $\mu\text{g}/\text{mL}$. Importantly, the mode of

cytotoxicity may differ at various concentrations, as the apoptotic and necrotic indexes increased depending on the AgNP concentration. However, at higher concentrations the necrotic effects became more dominant, with a minimal number of apoptotic figures. Gopinath et al. (2008) also previously proposed an apoptotic effect on cancer and normal cells in vitro induced by AgNPs used at low concentrations.

AgNPs induce cell responses often specific to cell types, resulting in varying degrees of toxicity. Depending on nanoparticle size, concentration, and exposure time, AgNPs induced different degrees of toxicity in vitro in fibroblasts, epithelial cells, melanoma cells, HaCaT cells, and HeLa cells (Pan et al., 2007; Park et al., 2007; Hess et al., 2008). Zanette et al. (2011) showed that AgNPs at a concentration of 11–36 $\mu\text{g}/\text{mL}$ caused a reduction in mitochondrial function. Similar results have been reported in human (0.5–3 $\mu\text{g}/\text{mL}$) and rodent (10–50 $\mu\text{g}/\text{mL}$) liver cells, alveolar macrophages (10–75 $\mu\text{g}/\text{mL}$), mouse dermal fibroblast cells and liver cells (30

µg/mL), and mouse germline stem cells (10 µg/mL) (Braydich-Stollen et al., 2005; Gopinath et al., 2008; Liu et al., 2010; Mahmood et al., 2010). An in vitro study by Sur et al. (2010) indicated that lactose-modified AgNPs enter A549 cancer cells at a higher rate compared to their entrance into L929 fibroblasts. Using an MTT assay, Liu et al. (2010) compared the effective concentration (EC₅₀) values of AgNPs of different sizes (~5 nm, ~20 nm, and ~50 nm) and surface areas on different cell types (A549, HepG2, MCF-7, and SGC-7901 cells). The cytotoxicity rate increased with the reduction of the AgNP size and increase of surface area. Furthermore, the cells tested by Liu et al. (2010) differed in cytotoxicity rate. For instance, the EC₅₀ value of AgNPs of ~20 nm in size in MCF-7 cells was 14.33 ± 0.561 µg/mL, while it was 50.94 ± 3.85 µg/mL in SGC-7901 cells. In our study, the size of AgNPs varied from 16 nm to 20 nm as determined by TEM and AFM studies. Using a WST-1 cytotoxicity test, we found that the IC₅₀ value was 40 µg/mL. We determined apoptotic and necrotic effects induced by AgNPs on MCF-7 cells even at a concentration as low as 10 µg/mL. Furthermore, the proliferation of MCF-7 cells was interfered with by AgNPs in a dose-dependent manner, starting at a concentration as low as 10 µg/mL. We think that the data generated through this study will be useful for our proposed future studies, in which we will focus on PPTT on MCF-7 cancer cell using AgNPs.

The mechanism of cytotoxicity induced by AgNPs is also of scientific interest to other researchers. AgNPs are reported to induce severe structural damage, accumulate in mitochondria, and contribute to oxidative stress (Asharani et al., 2009). Zanette et al. (2011) showed that AgNPs at a concentration of 11–36 µg/mL caused a reduction in mitochondrial function. Similar results have been reported in human and rodent liver cells, alveolar macrophages, mouse dermal fibroblast cells and liver cells, and mouse germline stem cells (Braydich-Stollen et al.,

2005; Gopinath et al., 2008; Liu et al., 2010; Mahmood et al., 2010). In addition, Oberley et al. (2006) reported that AgNPs reduced glutathione levels and increased generation of reactive oxygen species (ROS) in cells of the respiratory system. It is well known that ROS are highly reactive and cause oxidative harm to DNA and cell enzymes (Turrens, 2003; Boonstra and Post, 2004). Generation of excessive intracellular ROS leads to apoptosis and necrosis (Asharani et al., 2009; Hackenberg et al., 2011), evidenced by the fact that an increase in ROS levels is correlated with massive DNA breakage and high levels of apoptosis and necrosis (Foldbjerg et al., 2009; Singh and Ramarao, 2012). However, the cytotoxic effects may be partially due to direct action of Ag⁺ ions released from AgNPs. Singh and Ramarao (2012) reported that AgNPs were uptaken by macrophages via receptor-mediated phagocytosis, and Ag⁺ ions were released from AgNPs. The free Ag⁺ ions consequently may interfere with several cytoplasmic structures and pathways, including mitochondrial functions inducing stress pathways and apoptosis. Thus, further studies are needed to illuminate the AgNP-induced apoptosis and necrosis from the perspective of ROS.

In the present study, we preferred to fabricate AgNPs of 80 nm in hydrodynamic diameter, which is a considerably smaller size for testing cytotoxicity. As previously reported by Sohaebuddin et al. (2010), nanosized AgNPs are more toxic than larger and microsized particles. In addition, the AgNPs that we fabricated in this study are quite cytotoxic despite their negative charge (–38.2 mV).

In conclusion, AgNPs of 80 nm in hydrodynamic diameter and with a zeta potential of –38.2 mV express cytotoxicity on the MCF-7 cell line with an IC₅₀ value of 40 µg/mL. Thus, they can be used in vitro at concentrations of up to 40 µg/mL. AgNPs induce apoptosis and necrosis at lower concentrations, but induce necrosis only at higher concentrations. Future studies are needed to reveal the mechanism of the apoptotic and necrotic effects of AgNPs.

References

- Ahmed M, Karns M, Goodson M, Rowe J, Hussain S, Schlager J, Hong Y (2008). DNA damage response to different surface chemistry of silver nanoparticles in mammalian cells. *Toxicol Appl Pharmacol* 233: 404–410.
- Asharani PV, Hande MP, Valiyaveetil S (2009). Anti-proliferative activity of silver nanoparticles. *BMC Cell Biol* 10: 65–79.
- Asharani, PV, Low Kah Mun G, Hande MP, Valiyaveetil S (2009). Cytotoxicity and genotoxicity of silver nanoparticles in human cells. *ACS Nano* 3: 279–290.
- Boonstra J, Post JA (2004). Molecular events associated with reactive oxygen species and cell cycle progression in mammalian cells. *Gene* 337: 1–13.
- Braydich-Stollen L, Hussain S, Schrand A, Schlager J, Hofmann M (2005). In vitro cytotoxicity of nanoparticles in mammalian germline stem cells. *Toxicol Sci* 88: 412–419.
- Chaloupka K, Malam Y, Seifalian AM (2010). Nanosilver as a new generation of nanoparticle in biomedical applications. *Trends Biotechnol* 28: 580–588.
- Chen X, Schluesener HJ (2008). Nanosilver: a nanoparticle in medical application. *Toxicol Lett* 176: 1–12.
- Cho K, Park J, Osaka T, Park S (2005). The study of antimicrobial activity and preservative effects of nanosilver ingredients. *Electrochim Acta* 51: 956–960.
- Foldbjerg R, Olesen P, Hougaard M, Dang DA, Hoffmann HJ, Autrup, H (2009). PVP-coated silver nanoparticles and silver ions induce reactive oxygen species, apoptosis, and necrosis in THP-1 monocytes. *Toxicol Lett* 190: 156–162.
- Gopinath P, Gogoi SK, Chattopadhyay A, Ghosh SS (2008). Implications of silver nanoparticle induced cell apoptosis for in vitro gene therapy. *Nanotechnology* 19: 075104.

- Hackenberg S, Scherzed A, Kessler M, Froelich K, Ginzkey C, Koehler C, Burghartz M, Hagen R, Kleinsasser N (2010). Zinc oxide nanoparticles induce photocatalytic cell death in human head and neck squamous cell carcinoma cell lines in vitro. *Int J Oncol* 37: 1583–1590.
- Hackenberg S, Scherzed A, Kessler M, Hummel S, Technau A, Froelich K, Ginzkey C, Koehler C, Hagen R, Kleinsasser N (2011). Silver nanoparticles: evaluation of DNA damage, toxicity, and functional impairment in human mesenchymal stem cells. *Toxicol Lett* 201: 27–33.
- Hess R, Jones L, Schlager JJ (2008). Unique cellular interaction of silver nanoparticles: size-dependent generation of reactive oxygen species. *J Phys Chem B* 112: 13608–13619.
- Hsin Y, Chen C, Huang S, Shih T, Lai P, Chueh P (2008). The apoptotic effect of nanosilver is mediated by ROS- and JNK-dependent mechanism involving the mitochondrial pathway in NIH3T3 cells. *Toxicol Lett* 179: 130–139.
- Hussain SM, Hess KL, Gearhart JM, Geiss KT, Schlager JJ (2005). In vitro toxicity of nanoparticles in BRL 3A rat liver cells. *Toxicol In Vitro* 1: 975–983.
- Johnston HJ, Hutchison G, Christensen FM, Peters S, Hankin S, Stone V (2010). A review of the in vivo and in vitro toxicity of silver and gold particulates: particle attributes and biological mechanisms responsible for the observed toxicity. *Crit Rev Toxicol* 40: 328–346.
- Kamphaus GD, Colorado PC, Panka DJ, Hopfer H, Ramchandran R, Torre A, Maeshima Y, Mier JW, Sukhatme VP, Kalluri R (2000). Canstatin, a novel matrix-derived inhibitor of angiogenesis and tumor growth. *J Biol Chem* 275: 1209–1215.
- Kim J, Kuk E, Yuk N, Kim JH, Park SJ (2006). Mode of antibacterial action of silver nanoparticles. *J Proteome Res* 5: 916–924.
- Kim YS, Song MY, Park JD, Song KS, Ryu HR, Chung YH, Chang HK, Lee JH, Oh KH, Kelman BJ et al. (2010). Subchronic oral toxicity of silver nanoparticles. *Part Fibre Toxicol* 7: 20–31.
- Kreuter J, Gelperina S (2008). Use of nanoparticles for cerebral cancer. *Tumori* 94: 271–277.
- Leopold N, Lendl B (2003). A new method for fast preparation of highly surface-enhanced Raman scattering (SERS) active silver colloids at room temperature by reduction of silver nitrate with hydroxylamine hydrochloride. *J Phys Chem B* 107: 5723–5727.
- Li GY, Osborne NN (2008). Oxidative-induced apoptosis to an immortalized ganglion cell line is caspase independent but involves the activation of poly(ADP-ribose)polymerase and apoptosis-inducing factor. *Brain Res* 188: 35–43.
- Liu W, Wu Y, Wang C, Li HC, Wang T, Liao CY, Cui L, Zhou QF, Yan B, Jiang GB (2010). Impact of silver nanoparticles on human cells: effect of particle size. *Nanotoxicology* 4: 319–330.
- Liu X, Lee PY, Ho CM, Lui VC, Chen Y, Che CM, Tam PK, Wong KK (2010). Silver nanoparticles mediate differential responses in keratinocytes and fibroblasts during skin wound healing. *Chem Med Chem* 1: 468–475.
- Mahmood M, Casciano DA, Mocan T, Iancu C, Xu Y, Mocan L, Iancu DT, Dervishi E, Li Z, Abdalmuhsen M et al. (2010). Cytotoxicity and biological effects of functional nanomaterials delivered to various cell lines. *J Appl Toxicol* 30: 74–83.
- Oberdörster G, Oberdörster E, Oberdörster J (2005). Nanotoxicology: an emerging discipline evolving from studies of ultrafine particles. *Environ Health Perspect* 113: 823–839.
- Oberley T, Sioutas C, Yeh JI, Wiesner MR, Nel AE (2006). Comparison of the abilities of ambient and manufactured nanoparticles to induce cellular toxicity according to an oxidative stress paradigm. *Nano Lett* 6: 1794–1807.
- Pan Y, Neuss S, Leifert A, Fischer M, Wen F (2007). Size-dependent cytotoxicity of gold nanoparticles. *Small* 3: 1941–49.
- Park S, Lee YK, Jung M, Kim KH, Chung N (2007). Cellular toxicity of various inhalable metal nanoparticles on human alveolar epithelial cells. *Inhal Toxicol* 19: 59–65.
- Singh N, Manshian B, Jenkins GJ, Griffiths SM, Williams PM, Maffei TG, Wright CJ, Doak SH (2009). NanoGenotoxicology: the DNA damaging potential of engineered nanomaterials. *Biomaterials* 30: 3891–3914.
- Singh RP, Ramarao P (2012). Cellular uptake, intracellular trafficking, and cytotoxicity of silver nanoparticles. *Toxicol Lett* 213: 249–259.
- Sohaebuddin SK, Thevenot PT, Baker D, Eaton JW, Tang L (2010). Nanomaterial cytotoxicity is composition, size, and cell type dependent. *Part Fibre Toxicol* 7: 22–44.
- Sonoda E, Sasaki MS, Buerstedde JM, Bezzubova O, Shinohara A, Ogawa H, Takata M, Yamaguchi-Iwai Y, Takeda S (1998). Rad51-deficient vertebrate cells accumulate chromosomal breaks prior to cell death. *EMBO J* 15: 598–608.
- Su J, Zhang J, Liu L, Huang Y, Mason RP (2008). Exploring feasibility of multicolored CdTe quantum dots for in vitro and in vivo fluorescent imaging. *J Nanosci Nanotechnol* 8: 1174–1177.
- Sur I, Altunbek M, Kahraman M, Culha M (2012). The influence of the surface chemistry of silver nanoparticles on cell death. *Nanotechnology* 23: 375102.
- Sur I, Cam D, Kahraman M, Baysal A, Culha M (2010). Interaction of multi-functional silver nanoparticles with living cells. *Nanotechnology* 21: 175104.
- Tan WB, Jiang S, Zhang Y (2007). Quantum-dot based nanoparticles for targeted silencing of HER2/neu gene via RNA interference. *Biomaterials* 28: 1565–1571.
- Tian, J, Wong KK, Ho CM, Lok CN, Yu WY, Che CM, Chiu JF, Tam PK (2007). Topical delivery of silver nanoparticles promotes wound healing. *Chem Med Chem* 2: 129–136.
- Tice RR, Agurell E, Anderson D, Burlinson B, Hartmann A, Kobayashi H, Miyamae Y, Rojas E, Ryu JC, Sasaki YF (2000). Single cell gel/comet assay: guidelines for in vitro and in vivo genetic toxicology testing. *Environ Mol Mutagen* 35: 206–221.
- Türk M, Rzaev ZMO, Kurucu G (2010). Bioengineering functional copolymers. XII. Interaction of boron-containing and PEO branched derivatives of poly(MA-alt-MVE) with HeLa cells. *Health* 2: 51–61.

- Turrens J (2003). Mitochondrial formation of reactive oxygen species. *J Physiol* 552: 335–344.
- van Engeland M, Nieland LJ, Ramaekers FC, Schutte B, Reutelingsperger CP (1998). Annexin V-affinity assay: a review on an apoptosis detection system based on phosphatidylserine exposure. *Cytometry* 31: 1–9.
- Wijnhoven SWP, Peijnenburg WJGM, Herberts CA, Hagens WI, Oomen AG, Heugens EHW, Roszek B, Bisschops J, Gosens I, Van De Meent D et al. (2009). Nano-silver – a review of available data and knowledge gaps in human and environmental risk assessment. *Nanotoxicology* 3: 109–138.
- Yoon K, Hoon B, Park JH, Hwang J (2007). Susceptibility constants of *Escherichia coli* and *Bacillus subtilis* to silver and copper nanoparticles. *Sci Total Environ* 373: 572–575.
- Zanette C, Pelin M, Crosera M, Adami G, Bovenzi M, Larese FF, Florio C (2011). Silver nanoparticles exert a long-lasting antiproliferative effect on human keratinocyte HaCaT cell line. *Toxicol In Vitro* 5: 1053–1060.